Research Square

Preprints are preliminary reports that have not undergone peer review.
They should not be considered conclusive, used to inform clinical practice,
or referenced by the media as validated information.

Fourier based classification of mesoscopic folds: Insights into structural architecture of the Wolmara area, Kumaun Lesser Himalaya, (India)

HARITABH RANA
Dr. Hari Singh Gour University
HAREL THOMAS
harelthomas@gmail.com

Dr. Hari Singh Gour University

Research Article

Keywords: Almora, Fourier analysis, fold morphometric, structure, Kumaun, Himalaya

Posted Date: August 24th, 2026

DOI: https://doi.org/10.21203/rs.3.rs-10596521/v1

License: This work is licensed under a Creative Commons Attribution 4.0 International License.
Read Full License

Additional Declarations: No competing interests reported.

Abstract

The Wolmara area, located within the Almora Group of the Kumaun Lesser Himalaya presents a structurally complex geological landscape that has been shaped by multiple phases of deformation and on-going tectonic activity. This region is flanked by the Main Central Thrust (MCT) and the Main Boundary Thrust (MBT), showcasing significant fold formations, including tight isoclinal (F1) and moderately tight (F2) folds, which are indicative of a series of compressional events. This study employs harmonic Fourier analysis on 64 mesoscopic fold profiles from the Wolmara area, facilitating a quantitative categorization of fold shapes based on the b_3/b_1 ratio indicating that the predominant fold types are categorized as “Almost Parabola” and “Between Semi-Ellipse and Parabola,” reflecting early to intermediate deformation stages under moderate compressive forces. Also, angular and tightly closed folds, i.e., “Almost Chevron” and “Sine Wave,” are associated with greater deformation intensity during later stages. Transitional forms like “Between Sine Wave and Chevron” and the uncommon “Between Box and Semi-Ellipse” imply localized or terminal deformation phases that may be related to faulting and varying stress conditions at later stages. The observed spatial distribution and morphometric variation of fold types point to an increasing stress condition where initial symmetrical folds have developed into more complex shapes due to increasing stress. The use of Fourier analysis in this study offers a solid framework for the objective interpretation of fold shapes, deformation intensity, and tectonic history. These findings provide significant insights into the structural framework of the Almora Group and contribute to the understanding of the broader geodynamic evolution of the Lesser Himalayan fold-thrust belt.

1. Introduction

The Kumaun Lesser Himalaya, situated within the Western Himalaya, is known for its complex and unclear structural characteristics [1–4]. It is bordered to the north by the Main Central Thrust (MCT) and to the south by the Main Boundary Thrust (MBT) [5]. The internal structural intricacies of the Lesser Himalaya include the presence of fold and thrust belts along with subsequent strike-slip faulting [6–7]. Studies carried by [8–11] opined that the Himalayan range is supported by a gently dipping regional detachment at depths of 15–20 km, along which a less competent sedimentary wedge has separated from a more competent crystalline basement. The Kumaun Himalaya developed through a general advancement of thrusting towards the foreland in the southern direction, accompanied by some reactivation along the MCT, MBT, and the Himalayan Frontal Thrust (HFT). Subsequent compression of bedding parallel foliation (S0//S1) led to the steepening of S0//S1 beds and the formation of steep reverse faults [7]. In the central region of the Kumaun Lesser Himalaya, the Almora Nappe is classified as a doubly folded syncline in lenticular shape, comprising the Ramgarh Group of rocks as its lower unit and the Almora Group of rocks as its upper unit [12–17] The Almora group of rocks are strongly metamorphosed and less mylonitized showing the psammitic and pelitic rocks types as phyllites, schists and gneisses up to sillimanite zone [4]. The maximum pressure temperature calculated for these rocks are 700 ° C and up to 8 Kbar pressure [12]. While the rocks of Ramgarh group expose rocks of green

schist facies which are highly sheared and occur mostly as mylonites and ultramylonites after schists and quartzites. The rocks of Ramgarh and Almora group of rocks have been deposited during the Paleoproterozoic era yielding U-Pb age of 1800 Ma, [18–19]. However, [7] provide a distinct analysis of the Ramgarh and Almora Thrust sheets within the Kumaun Lesser Himalaya. They developed balanced cross-sections utilizing well log and seismic data from earthquakes in the Kumaun and Garhwal Himalaya, indicating that the Ramgarh thrust sheet acts as a horse situated beneath the Almora thrust sheet (Almora Group). Previous studies carried out on the NAT and SAT mainly focus on the petrotectonic history in the parts of the Almora nappe, inferring the maximum temperature of 500 to 600°C [5, 20–22, 12]. [12] inferred that the generally accepted framework of inverted metamorphism concerning the Himalayan metamorphic is not relevant to the central areas of the Almora Nappe. Therefore, thermal inversion appears to be a phenomenon specifically linked to thrust movements that occurred during the Himalayan orogeny, with only the lower sections of the Almora Nappe reflecting this occurrence, while large areas of the nappe remain unaffected by inverted metamorphism. Structural overview and tectonic disposition of the Almora group of rocks have been carried out by [12, 20, 23–24].

The rocks of the Almora group are exposed in the study area of Wolmara, Fig. 1. The area under investigation has undergone repeated phases of folding and faulting. The superposed mesoscopic structures also reveal that the area under investigation has suffered polyphase deformation [25–27]. The different folds developed in the area have been studied with the help of harmonic Fourier analysis. Fourier analysis is primarily utilized to identify the configurations of fold profiles, which were applied in this study to deduce the tectonic framework of the Almora group of rocks.

The application of the Fourier series in the study of geological folds has a historical precedent. [28] proposed this methodology in 1963, and it has been further explored through various methods and applications by researchers [29–36]. In nature, folds are typically observed at their final developmental stage. To investigate the progressive formation of folds, [33, 37] conducted experiments using physical models. Their research demonstrated that folds can transform through various shapes during their growth. [33] used a shear box and Ethyl cellulose for his experimental model, discovering that the strata began folding into a sinusoidal shape, which subsequently transformed into parabolic and semi-elliptical shapes as stress levels increased. Meanwhile, [37] used Plasticine for their experimental setup. Their laboratory investigation progressed through four stages, each defined by a distinct fold shape. The first stage was characterized by a chevron-sinusoidal shape, while the second and third stages exhibited nearly sinusoidal and parabolic shapes, respectively. The fourth stage culminated in a shape resembling a semi-ellipse, with hinge zones becoming more rounded as stress intensified, eventually achieving a box-like appearance. Further, this methodology was adopted by [38] for drawing the fold profile sections from the greenstone belts of Zimbabwe. In Indian context, studies have been carried out in the Kumaun lesser Himalaya at North Almora thrust (NAT) by [25–26, 34–35, 39–41]. [34] examined the North Almora Thrust region, focusing solely on the distinctions between the fold profiles of para-autochthonous and allochthonous rocks. Additionally, [35] carried out a study in central India, where they analyzed the Index of Non-Harmony (INH) using Fourier analysis and categorized the folds in the area

based on this index.[42] carried out strain analysis using the fold flattening methods for Aravalli rocks exposed around village Maruwas, Udaipur district, Rajasthan.

2. Local Geology and Structure

The Wolmara area (longitude 79°09'00” E to 79°17'56" E and latitude 29°47'42"N to 29°56'69"N), covering an area of about 120 km^2 is situated in District Almora, Uttarakhand, and can be approached by road from Kathgodam, which is the nearest railway station. The lithological units vary in their thickness, and due to intermittent outcrops, partly covered by the alluvial/soil and dense vegetation, it is difficult to show each unit on a geological map. Hence, individual units are grouped into three major lithological units i.e., phyllites, schists, and gneisses, for representation on the geological map (Fig. 2).

Figure 2a: Geological map around Wolmara, Kumaun Lesser Himalaya, Uttarakhand, India (modified after [43]).

Phyllites of the area are highly folded. Refolded structure and overturned folds in phyllites are exposed at several places and can be easily seen on the motor road leading to Udaipur around Chachroti, Galigaon, Kueta, and from Ruchaikhal to Pipalkhal. Gentle folds, asymmetrical folds, and chevron folds in phyllites, shown in Fig. 3a, c, are widely observed in the study area. Along with all these, ptygmatic folds are also found associated within phyllites. Chevron folds are commonly observed in this rock type (Fig. 3a). Phyllites showing gentle folds are exposed along the road to Kueta village (Fig. 3b). Single layer folds of quartz and first-generation tight isoclinal folds (Fig. 3c) have also been observed in these phyllites. Phyllites are commonly traversed by quartz veins which run parallel to schistosity. The folding of the quartz vein along with the schistosity has also been observed near the village Kueta. These phyllites exhibit well-developed crenulations. The phyllites of the area under investigation show a strike variation from NNE-SSW to WNW-ESE dipping towards northern and southern directions [13–17].

Figure 3a: Tight isoclinal fold exposed near Deghat village

Figure 3b: Folded quartz vien intruded in gneiss, near Papariya village

Figure 3c: Asymmetrical fold exposed near Chachroti village

Figure 3d: Gentle fold exposed along Pipalkhal village

Figure 3e: Gentle fold exposed along Kueta village

Figure 3f: Chevron fold exposed near Birot Village

3. Methodology

Fourier (Harmonic) analysis has been used to study the different folds of the area. The technique of Fourier or harmonic analysis is to use a series of simple x-y functions in mathematics to study the

curvature variation. Fourier (harmonic) analysis is a very simplified graphical method of plotting fold shapes on a two-dimensional graph. The Fourier analysis consists of a series of trigonometric functions to express the slope of any curve, which is as follows:

$f(x, y) = a_0 + a_1 \cos X + a_2 \cos 2X + a_3 \cos 3X + \ldots\ldots\ldots b_1 \sin X + b_2 \sin 2X + \ldots.$

“a” and “b” are various parameters called Fourier coefficients, representing the amplitude of the various cosine and sine components. A section of complete fold layer between an inflexion (i) line and hinge (h) line is selected. The “y” coordinate axis is chosen in such a way that it passes through the inflexion point, making it parallel to the fold axial surface. In a similar way, the “x” coordinate axis is made to pass through the inflexion point and perpendicular to the “y” coordinate axis so that it originates from point I, Fig. 4a-c. With this coordinate frame, all the “a”-type Fourier coefficients become zero, and the “b” -type Fourier coefficient can be represented in the function. Due to this, the changes in the shapes of successive quarter wave sectors go to make it zero, making the reduced Fourier series to represent the fold sector as:

$f(x,y) = b_1 \text{ Sin } X + b_3 \text{ Sin } 3X + b_5 \text{ Sin } 5X + \ldots\ldots\ldots.$

It is clear that the successive coefficients in this series become smaller, and in mathematical terminology, the series converges very rapidly. Only the first three coefficients provide significant input into the description of the wave shape, and the third of these takes on a very small value. The length of the line defining quarter wave base (W) is first measured and divided into three equal parts. A normal on each trisecting point of the quarter wave baseline is drawn so that it cuts the curved sector of the fold. The length of each of the three normal D_1, D_2 and D_3 is measured, Fig. 5a-b. The quarter wave base (W) is then converted into “π/2” units by dividing “π/2" by W. The parameters Y_1, Y_2 and Y_3 are then calculated by multiplying ($x = \pi/2/W$) with D_1, D_2 and D_3 respectively as follows:

$Y_1 = D_1 * X$

$Y_2 = D_2 * X$

$Y_3 = D_3 * X$

Where $X = (\pi/2W)$

Stableber (1968) has proposed that Fourier coefficient b_1, b_2 and b_3 can be calculated by using $X = (\pi/2/W)$ as follows:

$B_1 = (Y_1 + \sqrt{3}Y_2 + Y_3)/3$

$B_2 = (2Y_2 - Y_3)/3$

$B_3 = (Y_1 - \sqrt{3}Y_2 + Y_3)/3$

From the above equation b_2 and b_3 are providing the principal features of the fold shape and the positive values of b_3 reduce the amplitude effect of b1, while negative values increase it [33], Fig. 4b. The other significant effect of the b_3 coefficient is to modify the shape of the sinusoidal b1 components. Positive values of b_3 broaden the hinge region and tend to produce box shape folds whereas negative values tend to steep and straighten the fold limbs producing chevrons like style [27].

The fifth (b_5) Fourier component/harmonic is very small and exerts very little geometric effect on the style. [27] has given a graphical method for plotting fold shapes by representing graphically b_1 as abscissa and b_3 as ordinate. Each fold shape has a characteristic b_3/b_1 ratio viz. Chevron, Sinusoidal, Parabolic, Semi-ellipse, and box folds have b_3/b_1 values as 0.11, 0.00, 0.037, 0.165, and 0.333, respectively [27], Fig. 5a-b. [37] conducted an experimental study on the gradual transformation of fold shapes throughout their development concerning ongoing deformation. Their findings indicated that initially, the fold shape resembles a chevron style, which subsequently evolves into sinusoidal, parabolic, semi-elliptical, and finally box shapes. This progression suggests that, in geological terms, box-shaped folds are older than the others, while chevron folds are comparatively the youngest. [27, 41] further modified the classification with replacement of cuspate fold by Lobate and developed a computer program in QBASIC, which calculates the parameters b_1, b^3 and b_5 and ratios of b_3 and b_1 directly assigning the class of fold shapes based on the values of b_3/b_1.

Table 1
The class of fold shapes on the basis of the value of the ratio b_3/b_1 [27]

Class of Fold Shapes	**Value of the ratio of b_3/b_1**
Almost Box fold	< 0.409 to > 0.333 and < 0.333 to > 0.311
Almost chevron fold	<-0.072 to >- 0.111 and <-0.111 to >-0.172
Almost Parabola	< 0.058 to > 0.037 and < 0.037 to > 0.025
Almost Semi-ellipse	< 0.205 to 0.165 and < 0.165 to > 0.115
Almost sine wave	< 0.0081 to > 0.00 and < 0.00 to > -0.0193
Between Box fold and Semi ellipse	< 0.333 to > 0.205
Between Semi ellipse and parabola	< 0.115 to > 0.058
Between sine wave and chevron fold	< − 0.0193 to > − 0.072
Between parabola and sine wave	< 0.025 to > 0.0081
Box fold	0.333
Chevron fold	-0.111
Lobate fold	<-0.172
Multiple fold	> 0.409
Parabola	0.037
Semi ellipse	0.165
Sine wave	0.000

Table 2
Given values of D_1, D_2, D_3, W and results obtained by program b_3/b_1 and fold types

S.N.	D_1	D_2	D_3	W	b_3/b_1	Fold Type
1	0.65	0.90	0.95	0.70	0.111	Between Semi-Ellipse and Parabola
2	0.25	0.55	0.65	0.30	-0.081	Almost Chevron Fold
3	0.15	0.50	0.55	0.30	-0.160	Almost Chevron Fold
4	0.20	0.37	0.40	0.25	0.000	Sine Wave
5	0.45	0.65	0.72	0.60	0.078	Between Semi-Ellipse and Parabola
6	0.15	0.20	0.25	0.60	0.067	Between Semi-Ellipse and Parabola
7	0.32	0.70	0.80	0.72	-0.069	Between Sine-Wave and Chevron Fold
8	0.30	0.45	0.55	0.75	0.031	Almost Parabola
9	0.65	1.15	1.20	0.85	0.026	Almost Parabola
10	0.20	0.30	0.35	0.60	0.047	Almost Parabola
11	0.65	1.20	1.30	1.00	0.000	Sine Wave
12	0.35	0.55	0.70	0.60	0.000	Sine Wave
13	1.05	1.10	1.15	0.30	0.231	Between Box Fold and Semi-Ellipse
14	0.30	0.40	0.42	0.60	0.127	Almost Semi-Ellipse
15	0.18	0.47	0.50	0.30	-0.094	Almost Chevron Fold
16	0.70	1.10	1.20	1.10	0.053	Almost Parabola
17	0.90	1.20	1.30	0.70	0.117	Almost Semi-Ellipse
18	0.30	0.50	0.55	0.60	0.029	Almost Parabola
19	0.60	0.85	0.90	0.90	0.101	Between Semi-Ellipse and Parabola
20	0.70	0.88	0.95	1.00	0.142	Almost Semi-Ellipse
21	0.08	0.11	0.12	0.35	0.102	Between Semi-Ellipse and Parabola
22	0.45	0.60	0.70	1.00	0.091	Between Semi-Ellipse and Parabola
23	0.30	0.60	0.65	0.95	-0.025	Between Sine-Wave and Chevron Fold
24	0.50	0.95	1.00	1.10	0.000	Sine Wave
25	0.20	0.35	0.40	0.60	0.000	Sine Wave
26	0.30	0.50	0.60	1.00	0.000	Sine Wave

S.N.	D_1	D_2	D_3	W	b_3/b_1	Fold Type
27	0.30	0.50	0.70	1.00	-0.054	Between Sine-wave and Chevron Fold
28	0.60	1.00	1.05	0.95	0.044	Almost Parabola
29	1.10	1.65	1.85	1.75	0.060	Between Semi-Ellipse and Parabola
30	0.30	0.50	0.60	0.70	0.000	Sine Wave
31	0.30	0.35	0.40	0.30	0.153	Almost Semi-Ellipse
32	0.35	0.55	0.60	0.35	0.053	Almost Parabola
33	0.30	0.85	1.00	0.50	-0.144	Almost Chevron Fold
34	0.50	0.85	0.95	0.80	0.017	Between Parabola and Sine-Wave
35	0.50	0.78	0.85	0.50	0.056	Almost Parabola
36	0.25	0.50	0.55	0.45	-0.030	Between Sine-Wave and Chevron Fold
37	0.50	0.70	0.80	0.50	0.080	Between Semi-Ellipse and Parabola
38	0.10	0.20	0.24	0.65	-0.058	Between Sine-Wave and Chevron Fold
39	0.20	0.35	0.40	0.50	0.000	Sine Wave
40	0.30	0.30	0.45	0.50	0.107	Between Semi-Ellipse and Parabola
41	0.20	0.40	0.48	0.75	-0.058	Between Sine-Wave and Chevron Fold
42	0.35	0.55	0.65	0.50	0.026	Almost Parabola
43	0.16	0.18	0.20	0.20	0.179	Almost Semi-Ellipse
44	0.30	0.60	0.75	1.20	-0.072	Between Sine-Wave and Chevron Fold
45	0.30	0.68	0.80	0.70	-0.088	Almost Chevron Fold
46	0.60	1.10	1.35	1.00	-0.039	Between Sine-Wave and Chevron Fold
47	0.25	0.50	0.60	0.85	-0.058	Between Sine-Wave and Chevron Fold
48	0.40	0.55	0.60	1.00	0.102	Between Semi-Ellipse and Parabola
49	0.46	0.65	0.70	0.60	0.096	Between Semi-Ellipse and Parabola
50	0.45	0.70	0.80	1.10	0.041	Almost Parabola
51	0.40	0.70	0.75	1.10	0.021	Between Parabola and Sine-Wave
52	0.20	0.40	0.50	0.80	-0.072	Between Sine-Wave and Chevron Fold
53	0.25	0.45	0.50	0.78	0.000	Sine Wave
54	0.08	0.12	0.15	0.55	0.023	Between Parabola and Sine Wave

S.N.	D_1	D_2	D_3	W	b_3/b_1	Fold Type
55	0.35	0.55	0.65	0.80	0.026	Almost Parabola
56	0.25	0.38	0.40	0.60	0.078	Between Semi-Ellipse and Parabola
57	0.22	0.35	0.40	0.45	0.033	Almost Parabola
58	0.45	0.68	0.80	1.00	0.041	Almost Parabola
59	0.25	0.49	0.51	0.80	-0.006	Almost Sine-Wave
60	0.40	0.65	0.70	1.30	0.045	Almost Parabola
61	0.45	0.70	0.80	1.00	0.041	Almost Parabola
62	0.30	0.50	0.55	0.50	0.029	Almost Parabola
63	0.30	0.55	0.65	0.40	-0.026	Between Sine-Wave and Chevron Fold
64	0.40	0.70	0.85	0.95	-0.020	Between Sine-Wave and Chevron Fold

4. Fourier analysis and structural architecture of Wolmara area

The Almora group of rocks is characterized by its intricately folded lithological units showcasing a progressive evolution of folds. Various types of folds, measuring from a few centimeters to several meters, can be found in the study area. These folds play a crucial role in comprehending the deformational processes affecting the rocks and the structural framework of the region.

The F1 folds are characterized as tight isoclinal first-generation folds that formed along the schistosity planes (S1) and are typically distinguished by variations in lithology. These folds emerged as a result of the initial significant folding event that affected the rocks in the study area. The S1 plane exhibits a moderate dip towards the south to southwest and runs parallel or subparallel to the axial plane of the F1 folds, with the strike of the F1 axial planes ranging from east-west to west-northwest-east-southeast (Fig. 3d). The greater thickness found in the hinge areas relative to the limbs points to the movement of quartzo-feldspathic material from the limbs toward the hinge zone, a phenomenon regulated by lithology and the conditions of significant ductile strain. The second generation of folds, known as F2 folds, generally arise from the limbs of the earlier F1 folds. These F2 folds are moderately tight and isoclinal, with axial planes that are coaxial with those of the F1 folds. The hinge thickness of F2 folds is usually greater than that of their limbs, but it is always less than that of the F1 folds. In the area under study, the F2 folds are somewhat less tight than the F1 folds, indicating a relatively diminished intensity of deformation compared to the F1 folds. Chevron folds exposed near Birot village, Fig. 3a, possess straight limbs, distinct angular hinges, and typically acute inter-limb angles, showcasing symmetric or slightly asymmetric configurations. Their axial surfaces are largely perpendicular to σ1. They are frequently observed in multilayered alternating competent and incompetent layers, which results in a blend of similar geometries in incompetent layers and parallel geometries in competent layers. Sixty-four

location of fold exposure from the Wolmara area have been collected for the current study. The collected data have been processed through the SFARF software, [44]. Sixteen classes of fold shape based on the values of the ratio of b_3/b_1 classified by [27] have been used, shown in table. 1. The obtained values of D_1, D_2, D_3, W and results obtained by program b_3/b_1 and fold types are shown in table. 2 and Fig. 6. Consequently, it is observed that the Wolmara folds majorly fall in nine classes according to the [27, 33] division. The process of determining the sequence of fold formation can be intricate. In this research, the authors have taken a systematic approach by examining various fold classifications alongside their corresponding b_3/b_1 ratios. These ratios provide valuable insights into the deformation types that occurred within the rocks, which can be associated with the geological processes that led to folding. The b_3/b_1 ratio reflects the fold's shape, with its value indicating the degree of deformation or asymmetry present; different fold types correspond to specific ranges of this ratio. A higher b_3/b_1 ratio typically indicates more symmetrical or regular shapes, such as parabolas and semi-ellipses, whereas a lower ratio is indicative of more intricate or sharp fold shapes, like sine waves and chevrons. By analyzing the variations in the b_3/b_1 ratio, we can deduce the developmental history of the folds in response to varying stresses within the Earth's crust. The formation sequence of folds likely adheres to a pattern where simpler, more symmetrical types emerge first, followed by the development of more complex and asymmetric folds as deformation progresses. The sectors representing nearly parabolic and those between semi-ellipse and parabolic shapes are the most prevalent, comprising the majority of the folds observed. Conversely, the sectors corresponding to nearly sine wave folds and those between box folds and semi-ellipses are the least frequent, with only one fold identified in each case. The findings indicate that the classifications proposed by [27, 33] are relevant to the fold structures analyzed in this study, with the majority of the observed folds fitting into nine of these establelished categories.

- **Almost parabola fold sector**: Sixteen-fold shapes resemble almost a parabola whose values of b_3/b_1 range from < 0.058 to > 0.037 and < 0.037 to > 0.025 showing the highest numbers. The observed folds exhibit a regular pattern, indicating their formation under relatively uncomplicated and less intense compressive forces. These structures likely signify an initial phase of deformation, during which the layers are still reacting to moderate compressional stress while maintaining a degree of symmetry. The folds display a relatively symmetrical and smooth appearance, implying early to moderate levels of compression. Although the rock layers have experienced bending, they have not yet undergone significant deformation. At this juncture, the stress applied is sufficient to alter the layers without resulting in sharp, angular bends.
- **Between Semi ellipse and parabola fold sector**: The fold shapes of between semi-ellipse and parabola show the second highest numbering to twelve, whose values of b_3/b_1 range from < 0.115 to > 0.058. The presence of these folds may reflect a transitional phase in which deformation has escalated, though the complexity of the folds remains relatively simple. It is probable that compressive forces are becoming more pronounced, while the layers still bend in a manner that retains some structural order. These folds are elongated compared to parabola folds, indicating a rise in compressive forces. The layers are bending more sharply, resulting in an oval or elliptical

form. This deformation likely takes place during a transitional stage, where the forces are still robust, but the folding has not yet achieved the distinct sharpness of sine wave or chevron formations. Although they resemble parabola folds, the increased strain may lead to a slight onset of plastic deformation in the rocks.

- **Between sine wave and chevron fold sector**: Twelve-fold shapes fall between sine wave and chevron fold with b_3/b_1 values ranging from < − 0.0193 to > − 0.072. This indicates a more advanced phase of deformation, during which increased compressive forces result in more complex folding patterns. The resulting shapes exhibit reduced symmetry and indicate a more disordered stress environment. Sine wave and chevron folds are marked by their distinct, angular characteristics. Such folds develop as compressive forces intensify, resulting in intricate deformation. Notably, chevron folds are typically found in rocks that possess greater brittleness and lower ductility.
- **Sine wave fold sector**: Nine numbers of folds falls in this category whose b_3/b_1 values are 0.00. Sine wave folds are often irregular and demonstrate sharp, wave-like distortions. This category of folds may reflect a subsequent stage of deformation, where compressive forces are maximized, resulting in considerable bending of the rock layers, which could be attributed to high levels of strain or localized shear forces.
- **Almost Semi-ellipse fold sector**: Five numbers of fold falls in this category whose b_3/b_1 values range from < 0.205 to 0.165 and < 0.165 to > 0.115. While these folds maintain an elliptical appearance, they are characterized by a greater degree of stretching and a lack of symmetry relative to earlier folds. This change may reflect on going deformation resulting from high pressure, with the asymmetry potentially signaling that the layers are starting to buckle under increased stress.
- **Almost Chevron fold sector**: Five numbers of folds fall in this category whose b_3/b_1 values range from <-0.072 to >- 0.111 and <-0.111 to >-0.172. Chevron folds are characterized by their distinct, sharp, and angular points, which generally form under conditions of significant deformation. These structures indicate the presence of substantial compressive forces, likely leading to extreme bending of the rock layers and resulting in pronounced, angular crests. They exemplify a condition in which deformation has attained its peak intensity, causing the rock layers to experience both sharp bending and fracturing.
- **Between parabola and sine wave fold sector**: The b_3/b_1 values of this class range from < 0.025 to > 0.0081. Three numbers of folds fall in this category. Folds within this classification may indicate a transitional stage bridging the more symmetrical parabola-type folds and the intricate sine-wave folds. These formations could represent intermediate phases of deformation, characterized by significant forces that have not yet reached the chaotic level necessary to create fully developed sine-wave or chevron-like structures.
- **Almost Sine wave fold sector**: The b_3/b_1 values of this class range from < 0.0081 to > 0.00 and < 0.00 to > -0.0193. Only one fold falls in this category. These folds display b_3/b_1 values that range from < 0.0081 to > 0.00 and from < 0.00 to >-0.0193, resembling sine-wave folds, though the extent of deformation is not as pronounced. This phenomenon may suggest a heightened level of stress,

albeit manifested in a less distinct wave-like structure, likely influenced by localized shear forces or conditions of high pressure.

- **Between Box fold and Semi ellipse fold sector**: The b_3/b_1 values of this class range from < 0.333 to > 0.205. Only one fold falls in this category. The b_3/b_1 values for this category fall between less than 0.333 and more than 0.205, suggesting that the folds display certain box-like characteristics, frequently representing more localized and irregular forms. This is likely the final stage of folding, where irregular and potentially localized deformations take place, possibly as a consequence of localized forces or faulting.

5. General sequence of formation

1. **Initial Stage (Early Deformation)**: Folds identified in the Almost Parabola and the areas situated between the Semi-Ellipse and Parabola demonstrate early folding resulting from moderate compressive forces. These folds are notably symmetrical and exhibit a smooth texture.
2. **Intermediate Stage (Increasing Deformation)**: The rise in compressive forces leads to the emergence of folds in the Between Sine Wave, Chevron, and Almost Semi-Ellipse sectors. Consequently, these folds begin to take on more irregular and complex forms.
3. **Later Stage (Intense Deformation)**: Within the Sine Wave and Chevron domains, the folds display a more pronounced sharpness and angularity, suggesting that the deformation has peaked as a result of significant compressive forces.
4. **Final Stage (Localized or Complex Deformation)**: The folds found in the transitional areas between the Parabola and Sine Wave, as well as between the Box Fold and Semi-Ellipse sectors, may reflect localized or irregular folding patterns, which could be a consequence of localized faulting or shear zones.

6. Discussion

Beyond the b3/b1 classification applied here, the broader literature on fold-shape analysis offers a useful frame for interpreting why the Wolmara folds cluster so strongly around the parabolic to semi-elliptical field rather than spreading evenly across all sixteen classes. The two-coefficient approach formalised by [32–33] was always understood as an approximation: [48] showed that a fold profile is more completely described by fitting families of mathematical curves (parabolas, ellipses, hyperbolas) directly to digitised profiles, while [45–46] extended this to conic-section and kinematic modelling of layer-parallel shortening. [47] attempted a more rigorous six-parameter description of asymmetric folds but found that natural fold populations frequently plot outside the geometrically permissible field of his diagram, underscoring that no single low-order harmonic scheme can capture every fold perfectly. Viewed against this backdrop, the dominance of "Almost Parabola" and "Between Semi-Ellipse and Parabola" categories among the Wolmara folds is consistent with what would be expected of a population still within the early-to-intermediate range of layer-parallel shortening, where curvature is well approximated by low-order harmonics; the comparatively fewer folds occupying the sine-wave and chevron fields likely

represent surfaces whose true shape is more angular than two coefficients alone can fully resolve, a limitation also noted by [38] for the Zimbabwe greenstone belt profiles.

The pattern of shape change from open, rounded forms toward tighter, more angular geometries recorded here parallels observations from other fold-thrust settings analysed with the same harmonic method. In the Zagros fold-thrust belt of western Iraq, [36] documented an analogous progression in which folds nearer the more intensely shortened parts of the belt trend toward chevron-like b3/b1 values, while folds in less deformed positions retain higher, more parabolic ratios; the authors linked this directly to the magnitude of layer-parallel shortening accommodated locally. A similar correlation between harmonic fold shape and shear intensity has been reported from the South Delhi Fold Belt of Rajasthan, where [49] combined Ramsay's thickness-based classification with Fourier shape analysis to show that folds caught within the Ranakpur Shear Zone are measurably tighter and more strongly modified than pre-existing folds outside it. In the East Iran orogen, [50] likewise used b1 and b3 coefficients alongside interlimb-angle and aspect-ratio parameters to differentiate folds formed during successive buckling phases, finding that fold tightness increased systematically with proximity to active strike-slip splays. Read together, these studies support treating the b3/b1 signature not merely as a descriptive label but as a proxy for the relative amount of shortening a given surface has absorbed, which lends independent support to the sequence proposed for the Wolmara area, where progressively sharper fold classes are inferred to mark progressively later or more intense increments of deformation.

The mechanical basis for this shape progression is well established in classical buckle-folding theory. [51] analysis of folding in stratified viscoelastic media, and [52–53] fluid-dynamic treatment of selective buckling in layered sequences, both predict that fold shape is governed jointly by the viscosity contrast between competent and incompetent layers and by the total amount of layer-parallel shortening accommodated. [33] confirmed experimentally that, for a fixed viscosity ratio, folds pass through a recognisable sequence from open sinusoidal buckles at low strain to tight, thickened, near-isoclinal forms at high strain, with limb attenuation and hinge thickening becoming pronounced as shortening proceeds. This is directly relevant to the Almora Group lithologies at Wolmara, where phyllites, schists and gneisses of contrasting competence are interlayered: the greater thickness observed in F1 hinge zones relative to the limbs, attributed in this study to quartzo-feldspathic material migration, is the geometric signature predicted by this buckling theory for layers deformed well beyond their initial fold-nucleation stage, and offers a mechanical explanation, independent of the Fourier statistics alone, for why hinge-thickened, tighter classes such as "Almost Chevron" and "Between Sine-Wave and Chevron" are concentrated among the F2 and later structures rather than the earliest folds recognised in the area.

At the orogen scale, the spatial association between tighter fold classes and inferred proximity to major thrusts is also consistent with regional strain-gradient studies from other parts of the Himalaya. [54] documented an increase in internal crystal-plastic strain magnitude toward the Main Central Thrust in the Lesser Himalayan sheets of Bhutan, interpreting this as evidence that strain intensifies structurally upward within individual thrust sheets as they are stacked toward the hinterland. If a comparable strain gradient operates across the Kumaun Lesser Himalaya, the co-occurrence of tight, chevron-to-sine-wave

fold classes with zones of inferred later or more localised deformation at Wolmara would be a mesoscopic expression of the same process that produces heightened penetrative strain approaching the MCT elsewhere in the orogen, rather than a phenomenon unique to this study area. The interlimb-angle scheme of [55] although not applied quantitatively here, offers an independent qualitative cross-check on this interpretation: folds that this study classifies as "Almost Chevron" or "Sine Wave" on the basis of their b3/b1 ratio would also be expected to show correspondingly small interlimb angles in the tight-to-isoclinal range under Fleuty's scheme, and a combined application of both methods in future work could help resolve cases where the harmonic classification alone is ambiguous.

Taken together, the correlation drawn here between the b3/b1 fold-shape distribution at Wolmara and (i) the mechanics of progressive buckle folding, (ii) comparable harmonic-analysis studies from other fold-thrust belts, and (iii) documented strain gradients elsewhere in the Himalaya strengthens the case that fold shape in this area is recording a genuine, geologically meaningful deformation history rather than an artefact of the classification scheme. It also points to a clear direction for future work: pairing the Fourier coefficients with independent strain and interlimb-angle measurements, and, where profile data permit, with more complete curve-fitting approaches such as those of [46, 48], would allow the tectonic sequence proposed for the Almora Group to be tested more rigorously against quantitative strain data of the kind now available from other Lesser Himalayan transects.

7. Conclusion

The interpretation of b_3/b_1 ratios and their associated fold types suggest that the folding processes in the Wolmara area developed progressively. The initial folds were characterized by smoother and more symmetrical forms, which evolved into more complex and angular shapes as the compressive forces intensified. This sequence reflects the escalating intensity of tectonic forces acting upon the rocks, culminating in highly deformed and localized fold types. The variety of fold types observed in the Wolmara region indicates a shift from moderate deformation, such as parabola folds, to more intense and localized deformation, including chevron and sine wave folds. As the compressive forces grew stronger, the folds became sharper, more angular, and increasingly complex, highlighting the intensity and duration of tectonic processes like continental collisions and mountain building.

Declarations

Acknowledgements: The authors thank the Head of Department of Applied Geology, Dr. Harisingh Gour Vishwavidyalaya, Sagar (M.P) for conducting present research work.

Funding: The authors should like to put on record their candid thanks to the Head, Department of Applied Geology, Doctor Harisingh Gour Vishwavidyalaya, Sagar (M.P.) and the Department of Science and Technology, New Delhi, India for providing facilities as PURSE- Phase -II for conducting present research work.

AVAILABILITY OF DATA AND MATERIALS: The datasets generated during and/or analysed during the current study are available from the corresponding author on reasonable request.

Clinical trial number: not applicable

ETHICAL APPROVAL: Not applicable. This study did not involve human participants or animal subjects.

CONSENT TO PARTICIPATE: Not applicable.

CONSENT TO PUBLISH: Not applicable.

Competing Interest Declaration

We wish to confirm that there are no known conflicts of interest associated with this publication and there has been no financial support for this work that could have influenced its outcome.

Credit authorship contribution statement

Haritabh Rana: Writing – original draft, Software, Investigation.

Harel Thomas: Writing – review & editing, Supervision.

References

1. Rupke J. Stratigraphic and structural evolution of the Kumaon Lesser Himalaya. Sed Geol. 1974;11(2–4):81–265.
2. Valdiya KS. An outline of the structural set-up of the Kumaun Himalaya. J Geol Soc India. 1979;20(4):145–57.
3. Patel RC, Adlakha V, Singh P, Kumar Y, Lal N. Geology, structural and exhumation history of the Higher Himalayan Crystallines in Kumaon Himalaya, India. J Geol Soc India. 2011;77(1):47–72.
4. Rana H, Thomas H. Petrochemistry and P–T path for garnet mica schists from Patharkhola, Almora. Discover Geoscience. 2026;4(1):262.
5. Valdiya KS. The two intracrustal boundary thrusts of the Himalaya. Tectonophysics. 1980;66(4):323–48.
6. Molnar P, Tapponnier P. Cenozoic Tectonics of Asia. Effects of a Continental Collision. Features of recent continental tectonics in Asia can be interpreted as results of the India-Eurasia collision. Science. 1975;189(4201):419–26.
7. Srivastava P, Mitra G. Thrust geometries and deep structure of the outer and lesser Himalaya, Kumaon and Garhwal (India). Implications for evolution of the Himalayan fold-and-thrust belt. Tectonics. 1994;13(1):89–109.
8. Seeber L, Armbruster JG. Some elements of continental subduction along the Himalayan front. Tectonophysics. 1984;105(1–4):263–78.

9. Seeber L, Armbruster JG, Quittmeyer RC. Seismicity and continental subduction in the Himalayan arc. Zagros Hindu Kush Himalaya Geodynamic Evol. 1981;3:215–42.
10. Baranowski J, Armbruster J, Seeber L, Molnar P. Focal depths and fault plane solutions of earthquakes and active tectonics of the Himalaya. J Geophys Res Solid Earth. 1984;89(B8):6918–28.
11. NI J, Barazangi M. Seismotectonics of the Himalayan collision zone. Geometry of the underthrusting Indian plate beneath the Himalaya. J Geophys Res Solid Earth. 1984;89(B2):1147–63.
12. Joshi M, Tiwari AN. Structural events and metamorphic consequences in Almora Nappe, during Himalayan collision tectonics. J Asian Earth Sci. 2009;34(3):326–35.
13. Rana H, Thomas H. Geology of the Wolmara area, Almora District, Uttarakhand (India). with special reference to the lithology and field relation. Bulletin of the Department of Geology; 2018. pp. 1–6.
14. Rana H, Thomas H, Soni A, Shukla S. Petrochemistry of Phyllites from Wolmara, Kumaun lesser himalaya with Reference to Tectonic Implications. Earth Planet Sci. 2023a;2(2):1–9.
15. Rana H, Thomas H. 2023b: Structural, Micro-Structural and Thermal Characterizations of Natural Garnet of Regions of Wolmara from the State of Uttarakhand of India. Bulletin of Pure and Applied Sciences-Geology, (1).
16. Rana H, Thomas H, Batri R. Geochemical characteristics and tectonic interpretation of garnet mica schists of Wolmara area in Kumaun Lesser Himalaya, Uttarakhand Himalaya, India. Mineralia Slovaca. 2023c;55(2):133–42.
17. Rana, H., Thomas, H., Bidolya, J., Soni, A., Batri, R., Shukla, S., … and Karki, A.(2024): Geochemical constraints on the petrogenesis of Wolmara gneiss, Kumaun Lesser Himalaya, India. Mineralia Slovaca, 56(2), 153–164.
18. Das A, Rawat S, Modak PV, A. and, Nag R. 1800 Ma Ramgarh Gneiss of Kumaun Lesser Himalaya–An example of Palaeoproterozoic magmatism in Columbia Supercontinent. Indian J Geosci. 2018;72(3):203–14.
19. Jain AK, Mukherjee PK. Major unconformity between two juxtaposed sedimentary belts of the Lesser Himalaya, as revealed from the U–Pb zircon geochronology. J Earth Syst Sci. 2023;132(2):72.
20. Agarwal KK. Tectonic evolution of the Almora crystalline zone, Kumaun Lesser Himalaya. A reinterpretation. J Geol Soc India. 1994;43(1):5–14.
21. Gairola VK, Singh RA. 1995: Microstructures and evolution of folds in SC-mylonites from Dudatoli-Almora crystallines of Garhwal Himalaya. Proceedings of the Indian Academy of Sciences-Earth and Planetary Sciences, 104, 509–521.
22. Agarwal KK, Bali R. 2008: Small-scale deformational structures as significant shear-sense indicators. An example from Almora Crystalline Zone, Kumaun Lesser Himalaya. Earth Sci India, 1.
23. Joshi LM, Pant PD, Kotlia BS, Kothyari GC, Luirei K, Singh AK. 2016: Structural Overview and Morphotectonic Evolution of a Strike-Slip Fault in the Zone of North Almora Thrust, Central Kumaun Himalaya, India. Journal of Geological Research, 2016(1), 6980943.

24. Mandal S, Robinson DM, Kohn MJ, Khanal S, Das O, Bose S. Zircon U-Pb ages and Hf isotopes of the Askot klippe, Kumaun, northwest India. Implications for Paleoproterozoic tectonics, basin evolution and associated metallogeny of the northern Indian cratonic margin. Tectonics. 2016;35(4):965–82.
25. Shrivastava HB, Thomas T. Deformation and strain studies in a part of crystalline zone around Shalde, Kumaun Himalaya. Calcutta: Procee. Seminar on Evolution of Precambrian Crust in India; 1990. p. 38.
26. Thomas T. Structural studies in and around Shalde, Kumaun Himalaya. Abs. Indore: Indian Science Congress; 1991. p. 24.
27. Thomas T. 1993: A study of structure and tectonics of the area around Tamadhaun, district Almora, U.P. unpublished Ph.D. Thesis.
28. Norris DK. Shearing strain in simple folds in layered media. Geol Soc Can Paper. 1963;63:26–7.
29. Harbaugh JW, Preston FW. Fourier series analysis in geology. University of Arizona, College of Mines; 1965.
30. Whitten ET. 1969: Trends in computer applications in structural geology. In Computer Applications in the Earth Sciences. An International Symposium Proceedings of a conference on the state of the art held on campus at The University of Kansas, Lawrence on 16–18 June 1969. Sponsored by the Kansas Geological Survey, International Association for Mathematical Geology, and University of Kansas Extension (pp. 223–249). Boston, MA. Springer US.
31. Chapple WM. A mathematical theory of finite–amplitude rock–folding. Geol Soc Am Bull. 1968;79(1):47–68.
32. Stable.R CL. Simplified Fourier analysis of fold shapes. Tectonophysics. 1968;6(4):343–50.
33. Hudleston PJ. Fold morphology and some geometrical implications of theories of fold developed. Tectonophysics. 1973;16:1–46.
34. Singh RA, Gairola VK. Fold shape analysis in the vicinity of North Almora Thrust in District Chamoli – Garhwal Himalaya. Himalayan Geol. 1992;3(2):111–6.
35. Srivastava V, Gairola VK. Classification of multilayered folds based on harmonic analysis. example from central India. J Struct Geol. 1997;19(1):107–12.
36. Al-azzawi NK, Numan NM. The Structural Development of Folds Shapes in the Western Zagros Fold/Thrust Belt of Iraq Using Fourier Analysis. Iraqi Natl J Earth Sci. 2019;19(2):26–0.
37. Ramsay JG, Huber MI. Modern structural geology. Folds Fractures. 1987;2:309–700.
38. Stowe CW. Application of Fourier analysis for computer representation of fold profiles. Tectonophysics. 1988;156:303–11.
39. Tripathi A, Gairola VK. Fold symmetry- a quantitative description. J Struct Geol. 1999;21:719–27.
40. Srivastava HB, Thomas T, Tripathi RN. Petrographical approach to strain estimation in deformed rock, an example from granitic gneiss of a part of Almora synform Garhwal, Lesser Himalaya. Mem Geol Soc India. 2003;52:427–46.

41. Thomas H, Thomas T. Fourier Shape of The Fold Developed around Tamadhaun, District Almora Using a Computer Programm. Gond. Geol. Magz., Advances in Precambrian of Central India. Special Volume. 2003;7:169–76.
42. Baunthiyal V, Shrivastava S, Sharma A. 2019: Strain History of Aravalli Rocks Exposed Around Village Maruwas, Udaipur District, Rajasthan. Proceedings of Recent Advances in Interdisciplinary Trends in Engineering and Applications (RAITEA).
43. Thomas T, Thomas H. 1992: Fold flattening and strain studies in a part of Almora Crystalline Zone, around Tamadhaun Kumaun Himalaya. Indian Min Eng J. 5–7.
44. Thomas H, Sujata S, ChandeL A. 2008: SFARF. Software for Classification of Fourier Shape of the Folds Around Tamadhaun, District Almora, Uttarakhand. Earth Sci India, 1.
45. Aller J, Bastida F, Toimil NC, Bobillo-Ares NC. The use of conic sections for the geometrical analysis of folded surface profiles. Tectonophysics. 2004;379(1–4):239–54.
46. Bastida F, Aller J, Bobillo-Ares NC, Toimil NC. Fold geometry: a basis for their kinematical analysis. Earth Sci Rev. 2005;70(1–2):129–64.
47. Twiss RJ. Description and classification of folds in single surfaces. J Struct Geol. 1988;10(6):607–23.
48. Bastida F, Aller J, Bobillo-Ares NC. Geometrical analysis of folded surfaces using simple functions. J Struct Geol. 1999;21(7):729–42.
49. Hatui K, Chattopadhyay A. Modification of pre-existing folds in a shear zone: A case study from Kumbhalgarh–Ranakpur area, South Delhi Fold Belt, Rajasthan, India: K. Hatui, A. Chattopadhyay. J Earth Syst Sci. 2020;129(1):126.
50. Rashidi A, Shafieibafti S, Nemati M, Ezati M, Gholami E, Mousavi SM, Derakhshani R. Flexural-slip folding in buckling phases of orogenic belts: insight into the tectonic evolution of fault splays in the East Iran orogen. Front Earth Sci. 2023;11:1169667.
51. Biot MA. Theory of folding of stratified viscoelastic media and its implications in tectonics and orogenesis. Geol Soc Am Bull. 1961;72(11):1595–620.
52. Ramberg H. Fluid dynamics of viscous buckling applicable to folding of layered rocks. AAPG Bull. 1963;47(3):484–505.
53. Ramberg H. Selective buckling of composite layers with contrasted rheological properties, a theory for simultaneous formation of several orders of folds. Tectonophysics. 1964;1(4):307–41.
54. Long S, McQuarrie N, Tobgay T, Grujic D. Geometry and crustal shortening of the Himalayan fold-thrust belt, eastern and central Bhutan. Bulletin. 2011;123(7–8):1427–47.
55. Fleuty MJ. (1964). The description of folds. *Proceedings of the Geologists' Association*, *75*(4), 461–492.

Figures

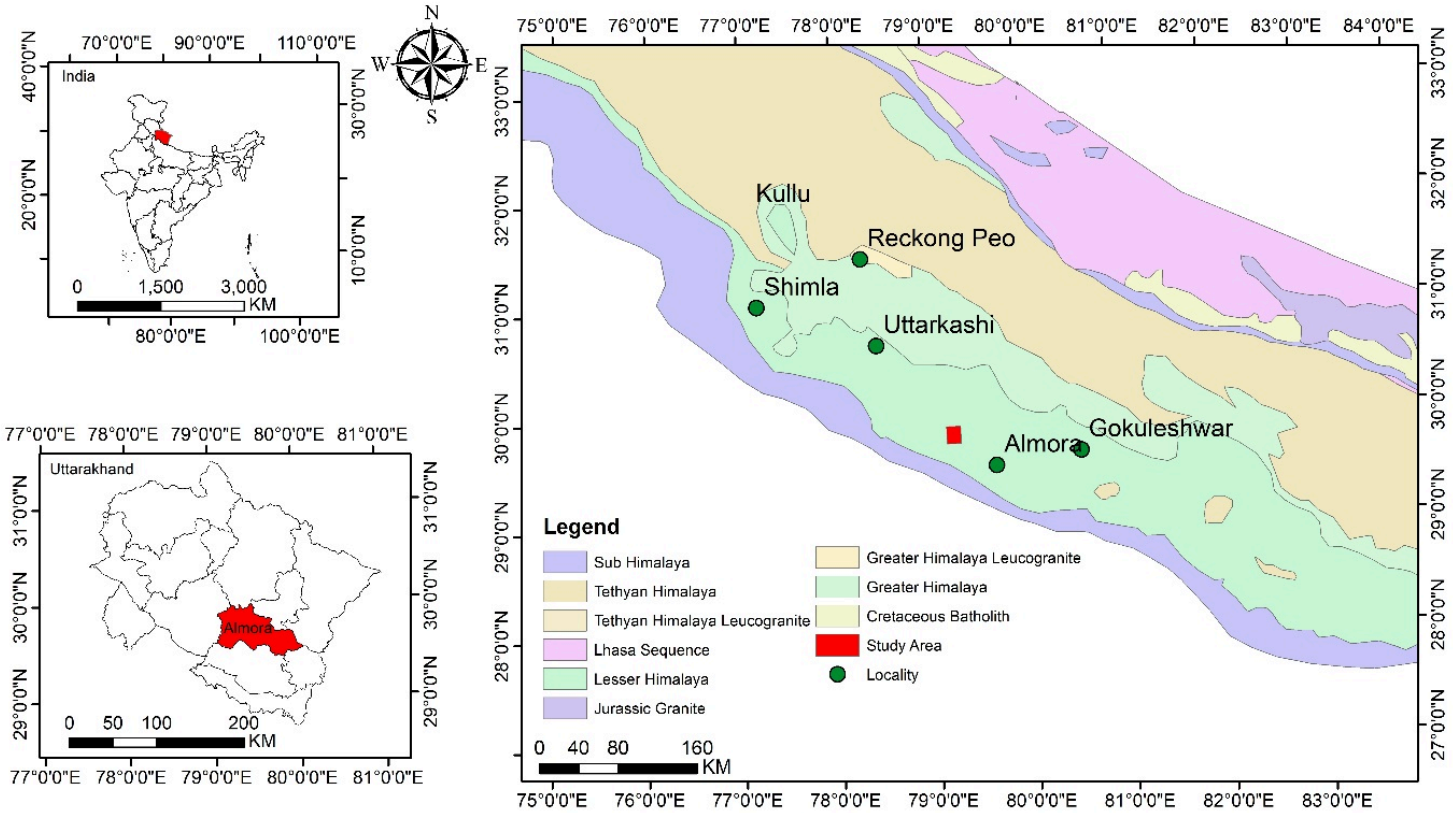


Figure 1

Simplified map of Himalaya (Modified after [4])

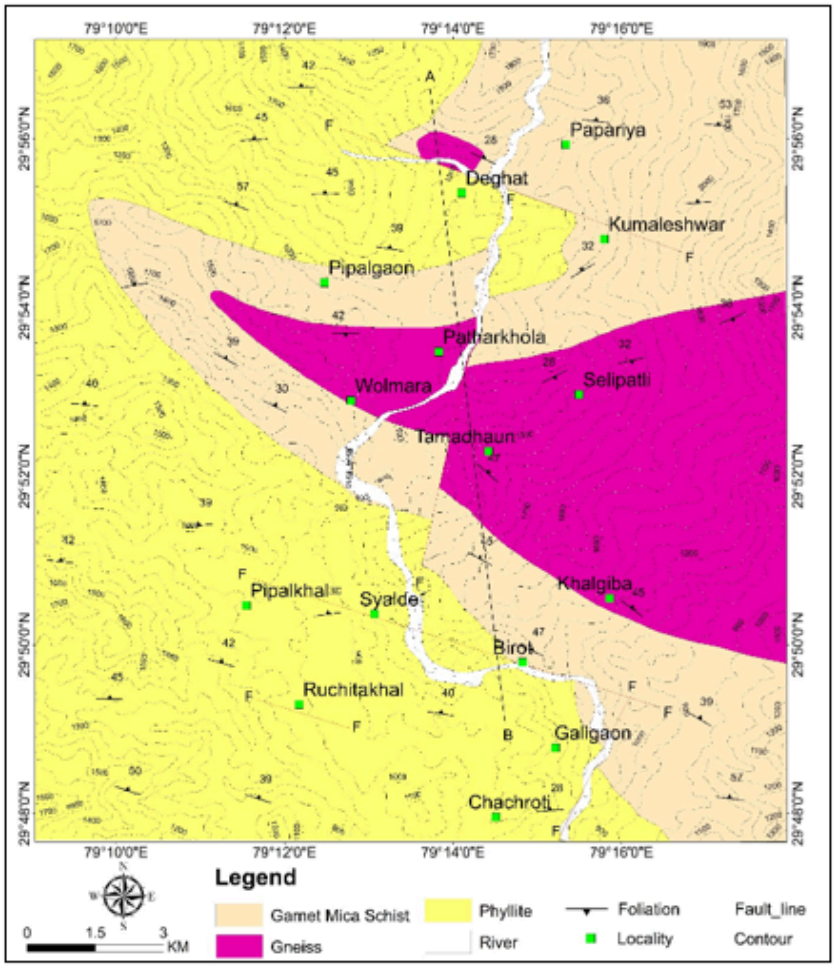


Fig. 2a:

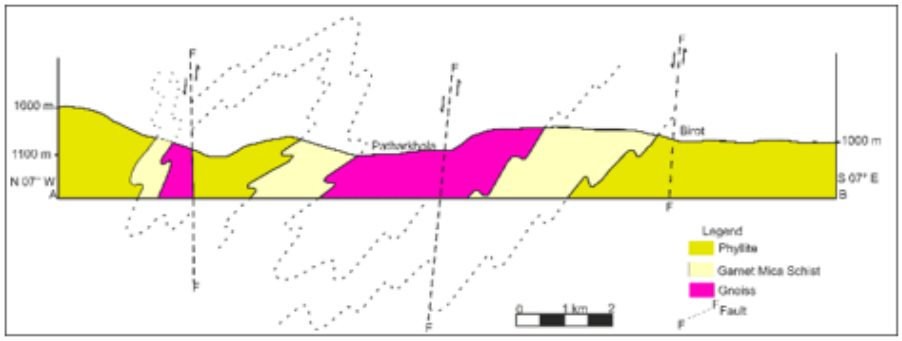


Fig. 2(b):

Figure 2

Fig. 2a: Geological map around Wolmara, Kumaun Lesser Himalaya, Uttarakhand, India (modified after [43]).

Fig. 2(b): Geological cross section of Wolmara area along A-B from north to south.

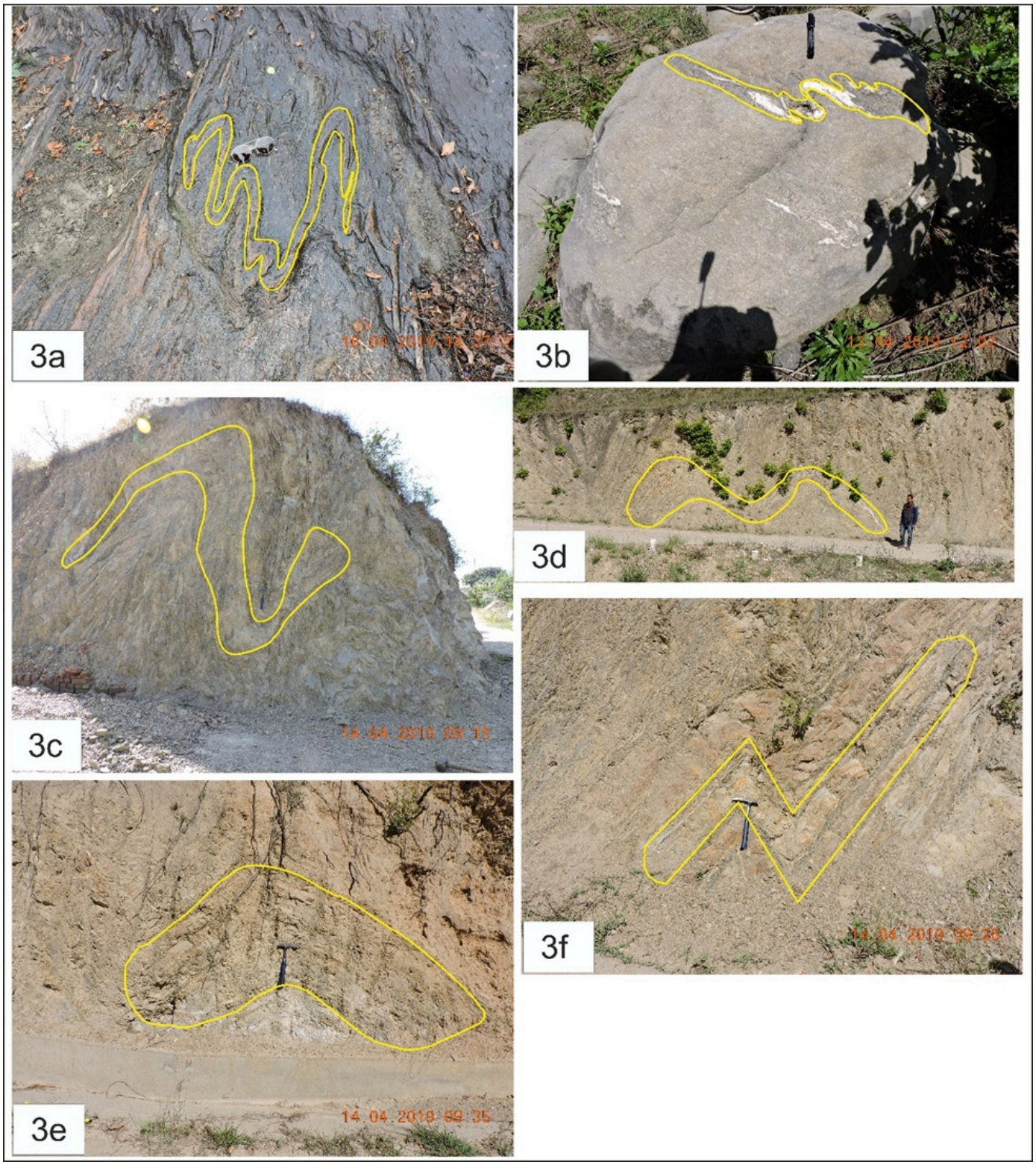


Figure 3

Fig. 3a: Tight isoclinal fold exposed near Deghat village

Fig. 3b: Folded quartz vien intruded in gneiss, near Papariya village

Fig. 3c: Asymmetrical fold exposed near Chachroti village

Fig. 3d: Gentle fold exposed along Pipalkhal village

Fig. 3e: Gentle fold exposed along Kueta village

Fig. 3f: Chevron fold exposed near Birot Village

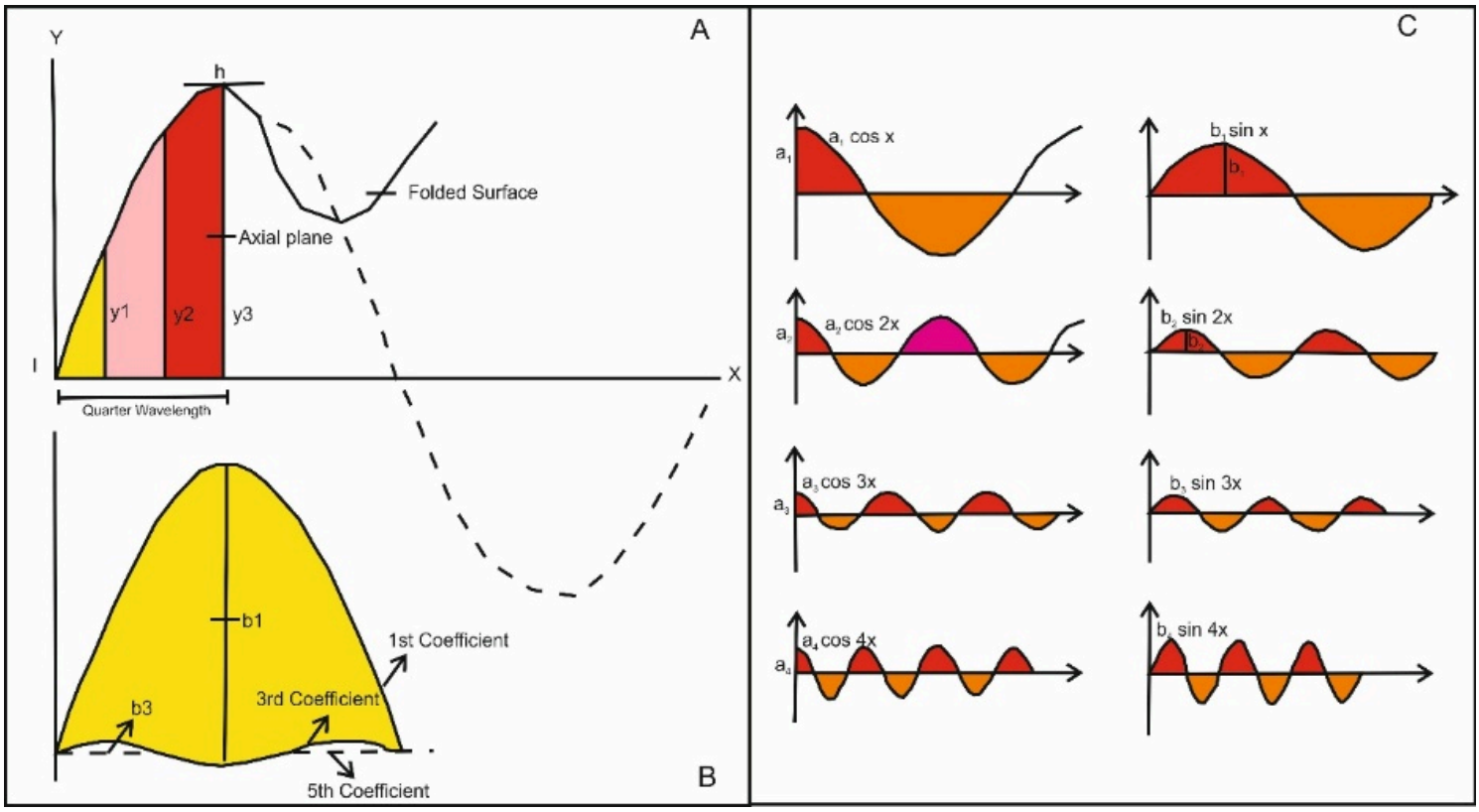


Figure 4

Fig. 4a: calculation of y_1, y_2 and y_3 for quarter wavelength; 4b: fourier coefficient location within folded layer; 4c: curves and functions of sines and cosines

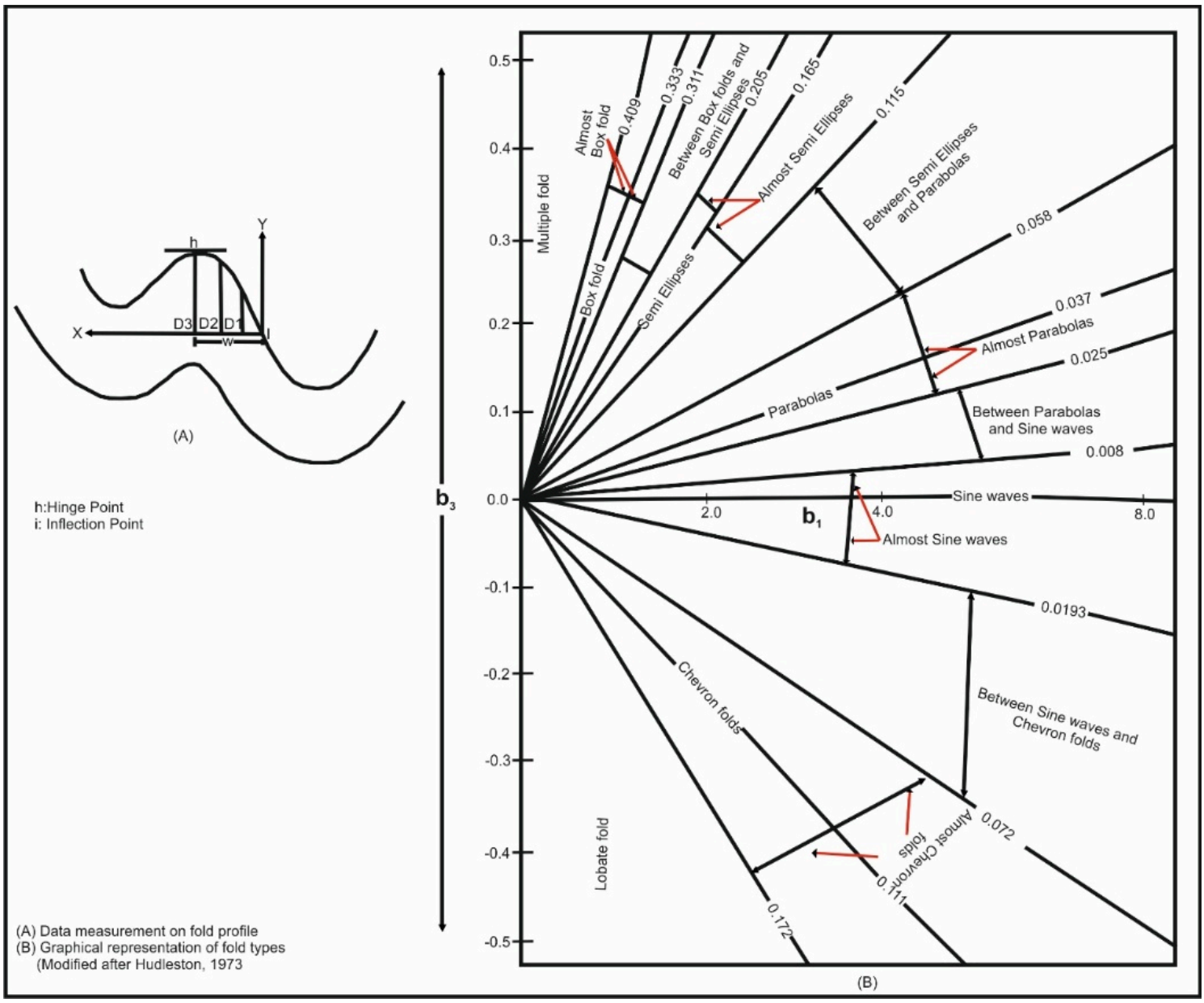


Figure 5

Fig. 5a: Data measurement on fold profile; 5b: Graphical representation of fold types (Modified after Huddleston, 1973)

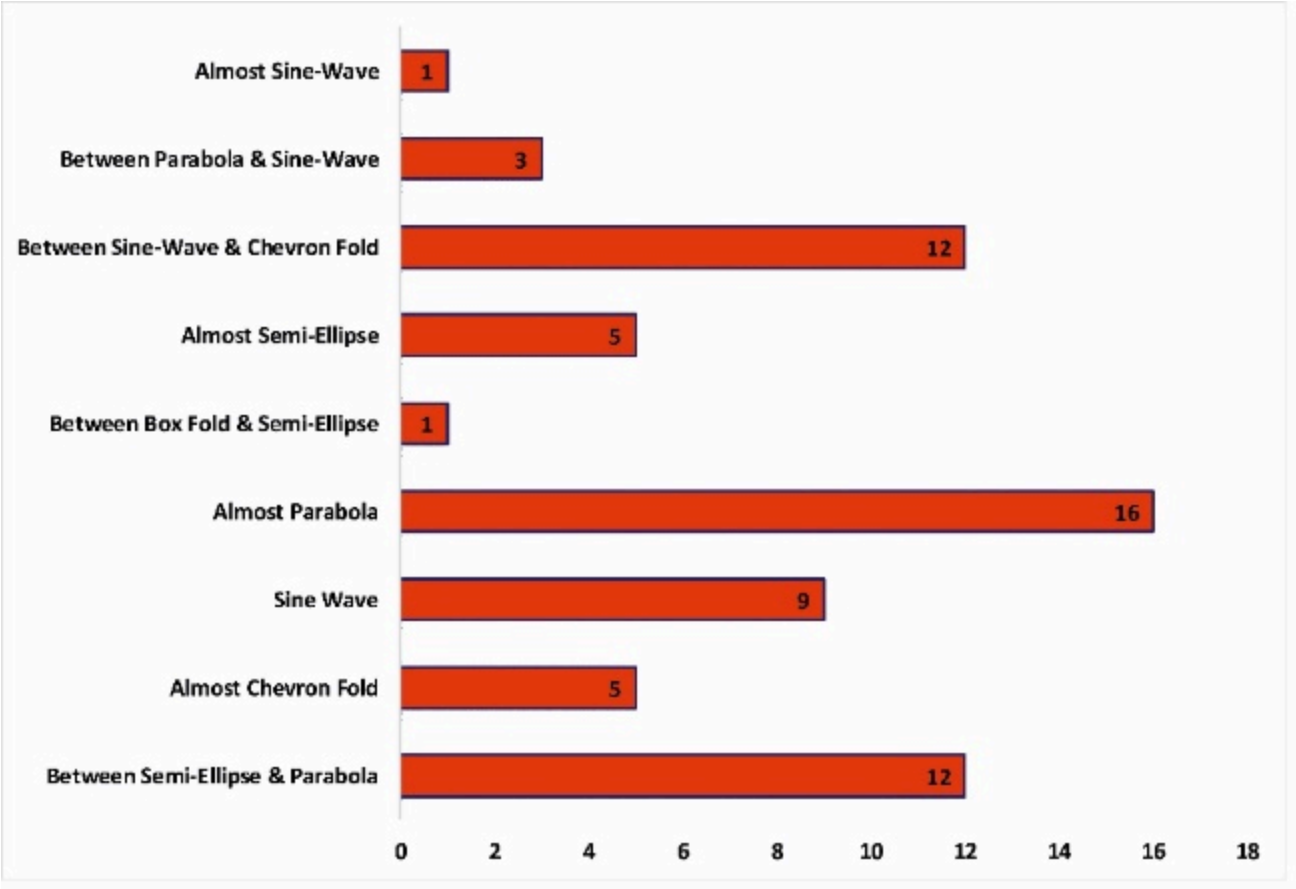


Figure 6

Frequency chart of various types observed in and around Wolmara area.